

## Zinc is Essential for the Copper Reductase Activity of Yeast Nucleosomes

Maria Vogelauer,<sup>1</sup> Chen Cheng,<sup>1</sup> Ansar Karimian<sup>1</sup>, Hooman Golshan Iranpour,<sup>1</sup> and Siavash K. Kurdistani<sup>1,2,3,4\*</sup>

<sup>1</sup>Departments of Biological Chemistry and <sup>2</sup>Pathology and Laboratory Medicine, David Geffen School of Medicine, University of California Los Angeles, Los Angeles, CA 90095, USA.

<sup>3</sup>Molecular Biology Institute, University of California Los Angeles, Los Angeles, CA 90095, USA.

<sup>4</sup>Eli and Edythe Broad Center of Regenerative Medicine and Stem Cell Research, David Geffen School of Medicine, University of California Los Angeles, Los Angeles, CA 90095, USA.

\* Correspondence to: [skurdistani@mednet.ucla.edu](mailto:skurdistani@mednet.ucla.edu)

**Author Contributions:** Conceptualization, M.V. and S.K.K; Methodology, M.V. and S.K.K; Investigation, M.V., C.C., A.K., H.G.I. and S.K.K.; Formal Analysis, M.V.; Writing – Original Draft: M.V. and S.K.K; Visualization, M.V.; Supervision, S.K.K.; Funding Acquisition, S.K.K.

**Competing Interest Statement:** The authors declare no competing interests.

**Classification:** Biological Sciences, Biochemistry

**Keywords:** Nucleosome, Chromatin, Histone, Copper reductase, Zinc.

## Abstract

The histone H3-H4 tetramer is a copper reductase enzyme, facilitating the production of cuprous ( $\text{Cu}^{1+}$ ) ions for distribution to copper-dependent enzymes. It was, however, unknown if this enzymatic activity occurred within nucleosomes. To investigate this, we obtained native nucleosomes from *Saccharomyces cerevisiae* using micrococcal nuclease digestion of chromatin in isolated nuclei and ion-exchange chromatographic purification. The purified nucleosomal fragments robustly reduced  $\text{Cu}^{2+}$  to  $\text{Cu}^{1+}$  ions, with the optimal activity dependent on the presence of zinc ions. Mutation of the histone H3 histidine 113 (H3H113) residue at the active site substantially reduced the enzymatic activity of nucleosomes, underscoring the catalytic role of histone H3. Consistently, limiting zinc ions reduced intracellular  $\text{Cu}^{1+}$  levels and compromised growth, phenotypes that were mitigated by genetically enhancing the copper reductase activity of histone H3. These results indicate that yeast nucleosomes possess copper reductase activity, suggesting that the fundamental unit of eukaryotic chromatin is an enzyme complex.

## Main Text

### Introduction

Histones help package eukaryotic DNA and regulate DNA-based processes such as gene expression (1). However, ancestral histones were present in organisms with small genomes, no nucleus and little ability for epigenetic regulation (2), suggesting that histones may have an additional, unknown function that could have served as the original impetus for their evolution. Inspired by geochemical events surrounding the appearance of the first eukaryotic cell, we have indeed discovered a novel function for histone H3 as a copper reductase enzyme, catalyzing the reduction of  $\text{Cu}^{2+}$  to  $\text{Cu}^{1+}$  ions (3). This reaction is important because copper must be in its reduced, cuprous state ( $\text{Cu}^{1+}$ ) for transport by copper chaperones such as Ccs1 and Atx1 to destination proteins.

Diminishing the copper reductase activity of histone H3 by mutating the critical histidine 113 residue at the active site to asparagine (H3H113N) reduced intracellular  $\text{Cu}^{1+}$  levels, leading to diminished function of copper-dependent enzymes such as complex IV of the mitochondrial transport chain or the super oxide dismutase 1 (Sod1) (3). Our data established a protein-based mechanism for regulating copper oxidation state inside the cell (3).

We have also recently provided the first example of how the copper reductase activity of histone H3 may contribute to the pathology of a human disease, namely, Friedreich's ataxia, a neurodegenerative disease caused by defective frataxin function (4). Frataxin is required for biosynthesis of iron-sulfur (Fe-S) clusters in mitochondria (5). Fe-S clusters serve as enzymatic or structural co-factors for a wide range of proteins (6). In the absence of frataxin function, the supply of Fe-S clusters declines, adversely affecting many metabolic and informational processes throughout the cell (7, 8). Since cuprous ( $\text{Cu}^{1+}$ ) ions are a main attrition factor for Fe-S clusters (9, 10), diminishing histone H3 copper reductase activity, hence intracellular  $\text{Cu}^{1+}$  levels, restored the functional pool of Fe-S clusters to a level that mitigated the phenotypes associated with their lower rate of

production (4). Our data suggested that the histone copper reductase activity may be a pathogenic factor in diseases in which Fe-S cluster homeostasis is altered (4).

A nucleosome is made up of a tetramer of histones H3 and H4, and two pairs of H2A-H2B dimers, which together wrap 146 bp of DNA (11). The histone H3-H4 tetramer is itself made up of two dimers of H3 and H4 histones which interact exclusively through histone H3 residues. The interacting H3-H3' interface is the suspected enzyme active site as it is where  $\text{Cu}^{2+}$  binds and is likely reduced. The assembly of histone H3 interface thus depends on the interaction of two H3-H4 dimers to form a tetramer. Two critical histone H3 residues at the interface, cysteine 110 (C110) and H113, are required for optimal  $\text{Cu}^{2+}$  binding and reduction *in vitro*. Interestingly, the histone H3 of the budding yeast as well as a few other fungi lack the C110 residue for reasons that are unclear. Our genetic analyses, however, suggested that despite lacking the C110 residue, the yeast histone H3 should also function as a copper reductase *in vivo* (3).

Previously we reconstituted the enzymatic activity of the Xenopus/human histone H3.2-H4 tetramer as well as the yeast H3-H4 tetramer containing a reintroduced C110 residue, from recombinant histones *in vitro* (3). In cells, the histone H3-H4 tetramer is found primarily in the nucleus and mostly in the context of a nucleosome (12), suggesting that it may function as a copper reductase within chromatin. Here, we provide evidence that the native yeast nucleosomes do indeed possess copper reductase activity; and the full activity depends on the presence of H3H113. We adapted a protocol for isolation of nucleosomes from the budding yeast *S. cerevisiae* to purify native nucleosomes of desired length with little RNA contamination (13). The protocol includes digestion of chromatin in isolated but otherwise intact nuclei using micrococcal nuclease (MNase) followed by an RNase treatment step. This releases nucleosomes of different lengths depending on the amount and length of MNase digestion, and substantially decreases RNA contamination. The released nucleosomes are then purified using ion-exchange chromatography. We then developed a modified copper reductase assay to demonstrate the enzymatic activity of native yeast nucleosomes *in vitro*. We also found that zinc ( $\text{Zn}^{2+}$ ) and cadmium ( $\text{Cd}^{2+}$ ), but not magnesium ( $\text{Mg}^{2+}$ ), calcium ( $\text{Ca}^{2+}$ ), manganese

(Mn<sup>2+</sup>) or nickel (Ni<sup>2+</sup>), ions are required for optimal copper reductase activity of wildtype nucleosomes. Mutation of the histone H3 histidine 113 (H3H113) residue at the active site substantially reduced the nucleosome enzyme activity. Consistently, deletion of *ZRT1*, the high affinity Zn<sup>2+</sup> transporter, decreased intracellular Cu<sup>1+</sup> levels when cells were grown in media with limited zinc ions and compromised growth. These phenotypes were rescued by a gain-of-function mutation in histone H3 that increases its copper reductase activity, providing strong evidence for the necessity of zinc ions for nucleosome enzyme activity in cells. Altogether, our findings suggest that the foundational unit of eukaryotic chromatin in yeast operates as a copper reductase enzyme complex and establish a functional link between zinc and intracellular copper oxidation states.

## Results

### **Purification of native nucleosomes from the yeast *Saccharomyces cerevisiae*.**

To obtain large amounts of native nucleosomes reproducibly, we adapted a protocol by Kuznetsov et al. for purification of native chromatin fragments (13). In our protocol (Fig. 1A), yeast cells were grown in rich media to logarithmically growing phase (log phase) and collected. Cell pellets were washed and pre-incubated in a buffer containing the reductant  $\beta$ -mercaptoethanol ( $\beta$ ME). Excess  $\beta$ ME was washed off and the cell wall was digested in an isotonic buffer by Zymolyase or Lyticase treatment to generate spheroplasts, which were then lysed in a buffer containing 18% ficoll to disrupt cell membrane but preserving nuclear integrity. The yeast nuclei were separated from cytoplasmic constituents using centrifugation, and subjected to MNase digestion. We empirically determined the amount and length of MNase digestion to generate mostly mono-, di- and tri-nucleosome chromatin fragments. We then added RNase A to the soluble chromatin to remove excess contaminating RNA.

We next used tandem chromatography consisting of inline cation-exchange and anion-exchange columns to purify native nucleosomes. The cation-exchange column eliminates

all positively charged molecules that could otherwise interact with DNA. Chromatin instead binds to the anion exchange column due to the negative charge of the DNA backbone that covers nucleosomes. The chromatography columns were then separated and nucleosomes bound to the anion-exchange column were eluted by a salt gradient. Figure 1B displays a representative chromatograph showing the elution profile of chromatin fragments. Gel electrophoresis of collected aliquots confirmed the fractions containing nucleosomes (Fig. 1C upper panel). Comparing a similar preparation but without the RNase A step revealed the critical importance of this RNA digestion step for increasing the yield and purity of isolated nucleosomes (Fig. 1S, compare to Fig. 1C upper panel). DNA extraction of the collected aliquots showed that DNA fragments of mostly mono-, di- and tri-nucleosomes co-elute with histones, as expected from a nucleosomal particle purification (Fig. 1C lower panel). Fractions containing nucleosomes were pooled and concentrated for further use.

We used Coomassie-stained gels to ensure equal amounts of nucleosomes are used when comparing assay conditions or nucleosomes isolated from different strains. Overall, our adapted protocol enables simple, rapid and reproducible isolation of native budding yeast nucleosomes of desired length containing little RNA contamination.

### **Copper reductase activity of nucleosomes *in vitro*.**

We next asked if the isolated nucleosomes reduce  $\text{Cu}^{2+}$  to  $\text{Cu}^{1+}$  ions *in vitro*. We adapted an assay that we have previously developed utilizing the bicinchoninic acid (BCA) chelator to detect  $\text{Cu}^{1+}$  production spectrophotometrically. Assays contained native nucleosomes or control buffer, reduced forms of tris(2-carboxyethyl)phosphine (TCEP) as electron donor and BCA in a potassium acetate buffer. Reactions were initiated by addition of  $\text{Cu}^{2+}$  in the form of  $\text{Cu}^{2+}$ -histidine complex. Spontaneous  $\text{Cu}^{1+}$  production occurred at a slow rate, but the rate of  $\text{Cu}^{1+}$  production substantially increased in the presence of wildtype (WT) chromatin (Fig. 2A). No significant production of  $\text{Cu}^{1+}$  occurred in the absence of TCEP, indicating that it, and not the nucleosomes or associated impurities, were the source of electrons (Fig. 2A). The nucleosomes also

reduced  $\text{Cu}^{2+}$  presented in complex with other small molecules such as serine (Fig. 2B). These findings suggest that the budding yeast native nucleosomes possess copper reductase activity *in vitro*.

### **Optimal copper reductase activity of native nucleosomes is dependent on zinc ions.**

Several alkali or transition metals including magnesium, calcium, manganese, nickel bind to nucleosomes and perturb the DNA or nucleosome structure in subtle ways (14, 15). The transition metal ion, zinc, is a co-factor for many transcription factors and enzymes in eukaryotes (16, 17). Interestingly, alterations in zinc levels are associated with changes in copper homeostasis in humans (18). To determine if metals have any effect on the nucleosome copper reductase activity, we performed the *in vitro* enzymatic assay in their presence. As shown in figure 2C,  $\text{Zn}^{2+}$  ions stimulated the copper-reductase activity of WT nucleosomes in a dose-dependent manner. This effect was highly specific as  $\text{Ca}^{2+}$ ,  $\text{Mn}^{2+}$ ,  $\text{Mg}^{2+}$  or  $\text{Ni}^{2+}$  had no effect on the nucleosomal reductase activity (Fig. 2D, 2E and S2A). Cadmium, however, with a valence electron configuration identical to zinc, also stimulated the copper reductase activity of nucleosomes (Fig. S2B), further supporting the specific nature of this stimulation

Commercially available Zymolyase, which we used to digest the cell wall, causes some clipping of the H3 N-terminal tail (13). To ascertain that nucleosomes containing full length H3 can also reduce  $\text{Cu}^{2+}$  ions, we prepared nucleosomes from spheroplasts obtained with recombinant Lyticase, which does not cause H3 tail clipping (13) (Fig. S2C, D). As observed with previous preparations, the resulting nucleosomes reduced copper, and their enzyme activity was stimulated by zinc (Fig. S2E). Zinc ions had no effect on the copper reductase activity of *Xenopus*/human histone H3.2-H4 tetramers (Fig. 2F), suggesting that the effects of zinc might be specific to nucleosomes.

We noticed three co-eluting bands in our nucleosomal fragment preparations (Fig. S2F). To ensure these bands were not the source of the observed enzymatic activity, we first employed mass spectrometry to discern their identities. As shown in figure S2G, these

bands correspond to the two largest subunits of the RNA polymerase II complex and a third band that comprises fragments of RNA polymerase II and potentially Ssa2, a subunit of the chaperonin-containing T-complex. Notably, none of these proteins have been previously associated with copper reductase activity. To further eliminate these proteins from consideration, we modified our nucleosome isolation procedure to incorporate an extensive wash with salt, significantly lowering the levels of the co-eluting bands (Fig. S3). We then pooled and concentrated several “pre-wash” fractions that predominantly contained the co-eluting proteins, with only minimal nucleosomes (Fig. S3B). Subsequent assessment of the copper reductase activity in both the “pre-wash” and nucleosomal fractions revealed that while the “pre-wash” fraction demonstrated minimal activity, the nucleosomal fraction exhibited substantially higher activity. These results collectively underscore that the enzymatic activity is inherent to the nucleosomes and is not a consequence of the co-eluting proteins.

### **Histone H3H113N mutation diminishes copper reductase activity of native nucleosomes.**

A pair of histidine residues (H3H113) at the H3-H3' interface is important for  $\text{Cu}^{2+}$  binding and reduction both *in vitro* and in cells (3). Mutation of H3H113 to alanine is lethal in yeast (19, 20). The lethality of H3H113A was previously ascribed to potential destabilization of the H3-H3' interface (21). However, introduction of C110 to yeast H3, which increases its copper reductase activity but does not contribute to H3-H3' interactions (11), rescued the lethality of strains carrying the H3H113A mutation (3). This finding indicated that diminished copper reductase activity may underlie the lethality associated with the H3H113A mutation. Guided by cancer-associated mutations in H3H113, we generated a yeast strain carrying the H3H113N mutation in both copies of histone H3 gene (3). Genetic analyses indicated that  $\text{H3}^{\text{H113N}}$  is a hypomorphic allele but may retain low but sufficient copper reductase activity to permit viability. Indeed, the yeast strains with H3H113N mutation have lower intracellular  $\text{Cu}^{1+}$  levels and display defects in the activity of copper-dependent enzymes. Consistently, the H3-H4 tetramers bearing the H3H113N mutation displayed lower copper reductase activity *in vitro* (3).

To ascertain if the H3H113N mutation also impairs the copper reductase activity of nucleosomes, we isolated nucleosomal chromatin fragments from the corresponding yeast strain (Fig. 3A) and determined their copper reductase activity in the presence of zinc. As expected, the H3H113N mutation markedly reduced the ability of nucleosomes to reduce  $\text{Cu}^{2+}$  (Fig. 3B), bringing it down to a level similar to the activity of WT nucleosomes in the absence of zinc (Fig. 3C). These results indicate that the enzymatic activity of yeast nucleosomes relies on the H3H113 residue, further supporting the catalytic role of histone H3 in copper reduction by nucleosomes.

### **Evidence for a role of zinc ions in regulating copper reductase activity *in vivo*.**

To provide *in vivo* evidence for the potential stimulatory effects of zinc on the enzymatic activity of nucleosomes, we deleted *ZRT1* (*zrt1Δ*), which encodes the high-affinity zinc transporter of the plasma membrane that is responsible for the majority of zinc uptake in yeast (22). We then grew WT and *zrt1Δ* yeast cells in low zinc media and assessed intracellular levels of  $\text{Cu}^{1+}$ . To do this, we used a reporter plasmid to read out the activity of the Cup2 transcription factor (Fig. 4A) (3). Cup2 is activated directly by  $\text{Cu}^{1+}$  and does not bind  $\text{Cu}^{2+}$  (23, 24). Importantly, neither Cup2 DNA binding nor its ability to activate transcription depends on zinc (24-26). The reporter plasmid harbors the GFP gene downstream of the CUP1 promoter, a main target gene of Cup2 (27, 28). Cells containing this plasmid displayed GFP expression proportional to the expected levels of cuprous ions in both physiological and genetic assays as previously reported (3). In both fermentative and oxidative media, GFP expression was higher in WT compared to *zrt1Δ* yeast cells. More strikingly, addition of excess copper to media increased the GFP signal dose-dependently in WT but much less so in *zrt1Δ* yeast cells, indicating that intracellular  $\text{Cu}^{1+}$  level is diminished when zinc ions are limiting (Fig. 4B and S4A). Because the reporter output depends on transcription, these data in fact indicate that  $\text{Cu}^{1+}$  levels are diminished in nuclei of *zrt1Δ* yeast cells. As expected, *zrt1Δ* cells grew worse compared to WT when zinc was limiting, both in fermentative and oxidative conditions (Fig. 4C

and S4B, left panel). Addition of copper abolished this growth difference (Fig.4C and S4B, right panel).

We further reasoned that increasing the copper reductase activity of nucleosomes should mitigate the hindering effect of low zinc levels. We previously showed that replacing histone H3 alanine 110 with cysteine (H3A110C), a residue that is present in the vast majority of eukaryotic histone H3 but missing in certain fungi (29), serves as a gain-of-function mutation, increasing the copper reductase activity of histone H3 (3). In *zrt1*Δ cells, the H3A110C mutation modestly but consistently increased intracellular Cu<sup>1+</sup> levels in oxidative conditions when demand for copper is high (Fig. 4D and Fig. S4C). Accordingly, the *H3<sup>A110C</sup>* yeast strain also grew more rapidly than WT in oxidative media with low, but not with replete, zinc levels (Fig. 4E and S4E), indicating that the effects of low zinc in diminishing Cu<sup>1+</sup> levels can be partially overcome by increasing the copper reductase activity of nucleosomes. This growth advantage of the *H3<sup>A110C</sup>* mutant was also evident in the absence of *ZRT1* (Fig. 4F). These data indicate that zinc levels influence intracellular Cu<sup>1+</sup> levels by modulating the enzymatic activity of chromatin.

## Discussion

We have previously established that the *Xenopus laevis* (Xl) histone H3-H4 tetramer, which is identical at the protein level to the human H3.2-H4 tetramer, possesses cupric reductase activity *in vitro*. We provided complementary genetic and molecular evidence that the yeast *S. cerevisiae* histone H3 may serve as a copper reductase in cells as well (3). However, the WT yeast H3-H4 tetramer does not seemingly assemble into the correct structure *in vitro*, precluding appropriate investigation of its potential copper reductase activity (3). The yeast histone H3 also lacks the H3C110 residue that is critical for the full enzymatic activity of the Xl/human histone H3-H4 tetramer. This left the question of whether the yeast histone H3, especially in the context of a nucleosome, functions as a copper reductase unanswered.

We now provide evidence that native yeast nucleosomes possess copper reductase activity *in vitro* and *in vivo*. These results provide further substantiation that the histone H3 functions as an oxidoreductase enzyme within nucleosomes, and that eukaryotic DNA is wrapped around an enzyme complex. We therefore submit that chromatin functions as a ‘metabolic organelle’ with its foundational unit harboring an oxidoreductase activity in eukaryotes.

We further show that among several transition metals,  $Zn^{2+}$  is specifically required for the optimal copper reductase activity of nucleosomes, and for nucleosome-mediated  $Cu^{1+}$  generation *in vivo*. Zinc is used as a co-factor for the function of hundreds of transcription factors and enzymes including histone deacetylases (30, 31). Certain enzymes such as Sod1 are dependent on both zinc and copper ions as cofactors (32). In multicellular organisms, including humans, the ratio of copper to zinc concentrations are tightly regulated. In human serum, changes in the ratio of copper to zinc have been linked to oxidative stress, inflammation and several age-related chronic conditions and diseases (18). Interestingly, zinc deficiency leads to hyperaccumulation of copper, yet a copper deficient phenotype in the green algae *Chlamydomonas* (33), which is consistent with decreased levels of intracellular  $Cu^{1+}$ . In assessing these relationships, the oxidation state of copper or a potential role for nucleosomes has not been considered. Nonetheless, dependence of the copper reductase activity of nucleosomes on  $Zn^{2+}$  ions may underlie the many known interactions between zinc and copper in eukaryotes. Considering that zinc levels could modulate copper oxidation state inside cells, the dependence of enzymes such as Sod1 on both copper and zinc and HDACs on zinc, raises the possibility of previously unrecognized regulatory mechanisms that integrate the activity of these enzymes not only to the availability of zinc and copper but also to the copper reductase activity of nucleosomes.

The mechanism underlying the enhancement of nucleosome copper reductase activity by zinc remains to be determined.  $Zn^{2+}$  ions are not known to undergo cycles of oxidation/reduction *in vivo* but could bind to DNA bases or the phosphate backbone (34-36). Oxidoreductase enzymes function by funneling electrons from regions of low to high

reduction potential but must avoid spurious discharge of electrons. By binding to DNA and/or histones,  $Zn^{2+}$  ions could provide structural support to nucleosomes to enhance their ability to extract electrons from donating co-factors and conduct them efficiently toward the  $Cu^{2+}$  bound at the active site. Interestingly,  $Zn^{2+}$  ions via binding to DNA bases can convert a stretch of DNA into a “molecular wire” capable of electron transfer (34). This raises the possibility that DNA may also participate in electron conductance for transfer of electrons from donor molecules to  $Cu^{2+}$  ions at the active site. Zinc has also been shown to potentially bind to or interact with the H3C110 residues at the active site (37). Although yeast histone H3 lacks C110, potential binding of  $Zn^{2+}$  ions to the active site could increase the off-rate of the  $Cu^{1+}$  product and thus enhancing the reaction. However, we do not favor such mechanism as  $Zn^{2+}$  would be expected to also enhance the activity of the H3-H4 tetramer, and in excess, to inhibit the enzymatic activity of nucleosomes—neither of which is borne out by our experiments.

The source of intracellular  $Zn^{2+}$  ions for nucleosome copper reductase activity remains to be identified. The levels of all metals, including  $Zn^{2+}$  ions, are tightly controlled, as too little would be insufficient for proper cellular function and too much could be toxic. Excess metals are typically bound by metallothioneins as a mechanism to prevent toxicity. Our data suggest that the levels of  $Zn^{2+}$  ions in the nucleus and their access to nucleosomes must be regulated in ways that were previously unsuspected. Our data, however, provide a regulatory basis for understanding how the interplay between intracellular levels of  $Zn^{2+}$ ,  $Cu^{2+}$  and  $Cu^{1+}$  vis-à-vis nucleosome-mediated copper reduction may affect the activity of many critical proteins and enzymes that rely on these metals for their function.

## **Materials and Methods**

### **Yeast strains and growth media.**

*Saccharomyces cerevisiae* strains used in this study are described in Supplementary Table 1. Fermentative and oxidative growth media is 0.17% yeast nitrogen base (Difco and Sunrise Science), 0.5%  $(NH_4)_2SO_4$  with either 2% dextrose (SC) or 2% EtOH/2% Glycerol

(SCEG), respectively, and supplemented with amino acids. Amino acid drop out mixes and metal free yeast nitrogen base were from Sunrise Science. Bacteria for histone expression were BL21(DE3) for histone H4 and Lyticase, and BL21(DE3) pLysS for histone H3 and were grown in 2xTY medium (1.6% Bacto Tryptone, 1% Yeast Extract, 0.5% NaCl) supplemented with 100µg/ml ampicillin or carbenicillin.

### **Strain generation for yeast experiments.**

*ZRT1* was deleted in WT (*OCY1131*) and H3<sup>A110C</sup> (NAY616) (3) cells using CRISPR-Cas9 as described in (38). Primers used to create the targeting plasmid are *zrt1*-pCAS9\_F (GGTCTTCCACACATCATCAGGTTTTAGAGCTAGAAATAGC) and pCAS9rev (pAAAGTCCCATTTCGCCACCCG). The resulting plasmid was then transformed together with the repair-template produced by primer extension of primers *dzrt1*REPF (ACTGCAAGTATAGACAATAAAACAACAGCACAAATATCAAAAAGGAATTA CCAAAGCGA) and *dzrt1*REPr (ATAAAATATGAAATAGAATCTATATGGAACATGCAGAATTTTCGCTTTGGTAA AAGGAATT). Successful deletion was verified by PCR.

### **Isolation of native nucleosomes from *Saccharomyces cerevisiae*.**

#### *Preparation of crude nuclei using commercial Zymolyase:*

For isolation of yeast nucleosomes, we adapted the protocol by Kuznetsov et al. (13) with some modifications. 1.5-3 liters (L) of yeast cells were grown in YPD to an OD<sub>600</sub> of 1.5, washed once with deionized water (ddH<sub>2</sub>O), and the wet weight of the pellet was determined. Cell pellets were then flash frozen and stored at -80°C. Cells were thawed and resuspended in 5 ml/g cells preincubation solution (0.7 M β-Mercaptoethanol, 2.8 mM EDTA) and incubated for 30 minutes at 30°C under constant agitation followed by one wash with 1 M Sorbitol. Cells were resuspended in 5 ml/g cells Zymolyase buffer (5 mM β-Mercaptoethanol, 1 M Sorbitol) and 2 mg/g cells of Zymolyase (MP Biomedicals) was added followed by incubation at 30°C for 30 minutes with constant agitation, and one wash with 1 M Sorbitol. The degree of spheroplastization was ascertained spectroscopically by comparing dilutions in ddH<sub>2</sub>O before and after Zymolyase treatment. Spheroplasts were resuspended in 5 ml/g cells Ficoll Solution (18% Ficoll, 20

mM KH<sub>2</sub>PO<sub>4</sub> pH 7.5, 1 mM MgCl<sub>2</sub>, 0.5 mM EDTA, 1x Protease inhibitors cocktail (Roche)) for cell lysis and crude nuclei were recovered by centrifugation at 30,000 rcf for 30 minutes at 4°C.

*Preparation of crude nuclei using recombinant Lyticase:*

Yeast cells were grown, harvested and frozen as described above. Pellets were thawed and resuspended in 10 ml/g pre-spheroplasting buffer (100 mM Tris-HCl pH 8, 60 mM β-Mercaptoethanol) and incubated rotating for 15 min at room temperature. Cells were then harvested and resuspended in 5 ml/g spheroplasting buffer (0.7 M Sorbitol, 0.75% Yeast Extract, 1.5% Peptone, 10 mM Tris-HCl pH 7.5, 10 mM β-Mercaptoethanol). Recombinant Lyticase was added at an empirically determined concentration and cells were incubated at 30°C for 15-20 min. Spheroplastization was ascertained spectroscopically by comparing cell densities of dilutions in either 1M Sorbitol or ddH<sub>2</sub>O. Preparation of crude nuclei was then continued as described above.

*Chromatin digestion:*

Crude nuclei were resuspended in 4 ml/g of cells in digestion buffer (1 M Sorbitol, 10 mM Tris-HCl pH7.5, 50 mM NaCl, 1 mM CaCl<sub>2</sub>, 5 mM MgCl<sub>2</sub>, 1 mM β-Mercaptoethanol and 1x Protease inhibitors cocktail) and equilibrated for 10 min in a 37°C water bath. Micrococcal Nuclease (MNase) (Sigma N5386) was diluted to 0.5 U/μl in MNase dilution Buffer (50% Glycerol, 50 mM Tris-HCl pH 8, 50 μM CaCl<sub>2</sub>). Crude nuclei were reacted with 5 U/g cells MNase at 37°C for 25 minutes. The reaction was quenched by addition of 1/4 volume of 5x quenching buffer (40 mM Tris-HCl pH 7.5, 2.45 M NaCl, 62.5 mM EDTA) and incubated on ice for 15 minutes to release chromatin fragments into solution. Chromatin was then cleared by centrifugation at 30,000 rcf for 30 minutes. The supernatant containing chromatin fragments was then treated with 6-10 μg/g cells DNase-free RNase (Roche) at 37°C for 30 minutes and subsequently cleared by centrifugation at 30,000 rcf for 30 minutes. This RNase step was critical for removing large amounts of contaminating RNA, which are likely ribosomal RNAs, to yield enzymatically active nucleosomes consistently.

### Nucleosome purification:

The cleared chromatin extract was then loaded onto a CM Sepharose FF HiTrap (Cytiva) mounted on top of a Q HP HiTrap (Cytiva) recursively at 4°C for 16 hours. Positively charged contaminating proteins were captured first by the CM Sepharose FF resin, while negatively charged DNA and chromatin bound to the anion exchange Q HP resin. The loaded Q HP HiTrap was then separated from the CM Sepharose FF HiTrap, washed with 20 column volumes of buffer A (5 mM Tris-HCl pH 7.5, 300 mM NaCl) and nucleosomes were eluted using twelve column volume (CV) salt gradient to reach 100% of buffer B (5 mM Tris-HCl pH 7.5, 750 mM NaCl). For Fig. S3, an initial gradient of nine CV up to 68% of buffer B (572 mM NaCl) was followed by two CV wash at 67% of buffer B (568 mM NaCl) to reduce the presence of proteins co-eluting with nucleosomes. The bulk of nucleosomes was then eluted by a three-CV gradient from 67% to 100% of buffer B. The peak of nucleosomes consistently eluted around 630 mM NaCl. Eluted aliquots were analyzed by polyacrylamide gel electrophoresis (PAGE) and nucleosomal fractions were pooled and concentrated using Amicon Ultra 15 with a molecular weight cutoff of 50K (Millipore). Salt concentration was then reduced by addition of 20 volumes of 5 mM Tris-HCl pH 7.5 followed by further concentration. The resulting nucleosomal preparation was aliquoted immediately and stored at -80°C. The resulting flow through was used as “buffer” control in subsequent experiments.

### **DNA extraction.**

50 µl of chromatin fractions or 20 µl of final nucleosomal sample were brought to 100 µl with ddH<sub>2</sub>O. 1 µg DNase-free RNase (Roche) was added and reacted for 30 minutes at 30°C. Proteins were then degraded by addition of 50 µg Proteinase K (Roche) and incubation at 56°C for 90 minutes, followed by DNA purification using a QIAquick PCR purification kit (Qiagen).

### **Copper reduction assay.**

5 µl of nucleosomes, corresponding to approximately 5 µg histones, or control buffer were diluted to a final reaction mixture containing 67 µM Tris-HCl pH 7.5, 50 mM KOAc, 0.5 mM bicinchoninic acid (BCA) (Sigma) and 50-100 µM TCEP (Sigma) pH

7.5, as indicated. Zinc was added in the form of ZnSO<sub>4</sub> where indicated. Magnesium, calcium and nickel were added as MgCl<sub>2</sub>, CaCl<sub>2</sub> and NiSO<sub>4</sub> where indicated. Reactions were then started by addition of a CuSO<sub>4</sub>-Histidine 1:1 or CuSO<sub>4</sub>-Serine 1:2 mix to a final concentration of 0.5 mM. Absorbance at 562 nm was measured every 0.5 seconds using a Hewlett-Packard HP8453 diode-array UV/Visible spectrophotometer.

### **Purification of recombinant Lyticase.**

A plasmid for the expression of recombinant Lyticase was kindly provided by Craig Peterson (pCP330). The plasmid was transformed into BL21(DE3) (Invitrogen) and 35 ml starter culture with 2xTY containing 100 µg/ml carbenicillin (Goldbio) was grown for 16 hours. A 1:100 dilution into 3 L of the same media was grown to OD<sub>600</sub> ~0.25 and induced with 0.4 mM Isopropyl β-D-1-thiogalactopyranoside (IPTG; Goldbio). Cells were harvested, washed once with 500 ml 25 mM Tris-HCl pH7.5 and finally stirred for 20 min in 80 ml 12.5 mM Tris-HCl pH 7.5, 1 mM EDTA, 20% sucrose and harvested again at room temperature. Cells were then resuspended in ice-cold 0.5 mM MgSO<sub>4</sub> and stirred on ice for 20 min. Cell debris was then pelleted at 4°C and the supernatant was dialyzed three times against 2 L of 50 mM NaOAc pH5.3, 1 mM EDTA, and 1 mM β-mercaptoethanol at 4°C. Precipitate was removed by centrifugation and the remaining lysate was further purified by cation exchange using a 5 ml HiTrap SP HP (Cytiva). Proteins were eluted by a gradient to 300 mM NaCl and Lyticase containing fractions were pooled, concentrated and flash frozen at -80°C. Activity of the enzyme was determined empirically.

### **Histone purification.**

Histone purification was performed as previously described (39) except that purification by size exclusion was omitted and the solubilized inclusion bodies were pre-cleaned by passage over a Hi-Trap Q-Sepharose column (GE Healthcare) before loading onto a Hi-Trap SP-Sepharose column (GE Healthcare). Histones were eluted by a salt gradient from 200 to 600 mM NaCl, as described previously (39), and fractions containing pure histones were pooled, dialyzed three times against 4 L of 2 mM β-mercaptoethanol (Sigma) in water, flash frozen and lyophilized.

### **H3-H4 tetramer assembly.**

H3-H4 tetramer assembly was performed as previously described (40) with some modifications. Briefly, equimolar amounts of H3 and H4 were dissolved in 7 M Guanidinium HCl, 20 mM Tris-HCl pH 7.5 and 10 mM DTT at a concentration of 1-2 mg/mL total protein. refolding was achieved by 1-2 hr dialysis at 4°C against 1 L of 2 M NaCl, 10 mM Tris-HCl pH 7.5, 1 mM EDTA, 5 mM  $\beta$ -mercaptoethanol (TEB), then 2 hrs against 1 L of 1 M NaCl - TEB, followed by 16 hrs against 0.5 M NaCl –TEB. The refolded tetramer was centrifuged for 5 min at 13000 rcf at 4°C to eliminate insoluble particles and purified by size exclusion chromatography on a HiLoad 16/600 Superdex 200 column (Cytiva) at 1 mL/min in 500 mM NaCl, 5 mM Tris-HCl pH 7.5. Fractions containing the tetramer were concentrated using Amicon Ultra–15/Ultracel-30K centrifugal filters (Millipore). The flow-through buffer was used as negative control (“buffer”) in the copper reductase assay.

### **Mass Spectrometry.**

Protein bands were excised from the gel and in-gel digested with trypsin according to a published protocol (41), with some modifications. A piece of gel cut from a blank region of the gel and processed in parallel with the sample, served as a control. Briefly, the gel pieces were destained, dehydrated and dried. The proteins in the gel pieces were reduced with 10mM dithiothreitol at 56°C followed by alkylation with 55 mM iodoacetamide at 25°C in dark. After washing, the gel pieces were subjected to dehydration by addition of acetonitrile, then rehydration in 50 mM  $\text{NH}_4\text{HCO}_3$  followed by dehydration again. The gel pieces were dried and rehydrated in 12.5 ng/ $\mu\text{L}$  of trypsin in 50 mM  $\text{NH}_4\text{HCO}_3$  at 4°C. After complete rehydration of gel pieces, the supernatant was removed and replaced with 50mM  $\text{NH}_4\text{HCO}_3$  buffer (without trypsin) and incubated at 37°C, overnight. Peptides were extracted from the gel matrix by two rounds of incubation in extraction buffer containing 5% formic acid and 30% acetonitrile. Following extraction, the gel pieces were dehydrated with acetonitrile. The supernatant was pooled with extraction buffer recovered from the previous step, dried and subsequently analyzed by LC-MS/MS.

Briefly, peptides were separated by reversed phase chromatography using 75  $\mu\text{m}$  inner diameter fritted fused silica capillary column packed in-house to a length of 25 cm with bulk 1.9  $\mu\text{M}$  ReproSil-Pur beads with 120 $\text{\AA}$  pores (42). The increasing gradient of acetonitrile was delivered by a Dionex Ultimate 3000 (Thermo Scientific) at a flow rate of 200 nl/min. The MS/MS spectra were collected using data dependent acquisition on Orbitrap Fusion Lumos Tribrid mass spectrometer (Thermo Fisher Scientific) with an MS1 resolution (r) of 120,000 followed by sequential MS2 scans at a resolution (r) of 15,000. The data generated by LC-MS/MS were analyzed on MaxQuant bioinformatic pipeline (43). The Andromeda integrated in MaxQuant was employed as the peptide search engine and the data were searched against *Saccharomyces cerevisiae* database (Uniprot Reference UP000002311). A maximum of two missed cleavages was allowed. The maximum false discovery rate for peptide and protein was specified as 0.01. Label-free quantification (LFQ) was enabled with LFQ minimum ratio count of 1. The parent and peptide ion search tolerances were set as 20 and 4.5 ppm respectively.

### **Flow cytometry.**

Single colonies of cells bearing the Cup2 reporter plasmid (3) were grown in liquid SC-ura media containing 0.25  $\mu\text{M}$  ZnSO<sub>4</sub> (“low zinc”) for 16 hrs to deplete endogenous zinc reserves. Cells are then washed twice with ddH<sub>2</sub>O and seeded at OD<sub>600</sub> 0.2 density in either low zinc SC-ura or low zinc SCEG-ura and 0, 1 or 10  $\mu\text{M}$  CuSO<sub>4</sub> was added. After 24 hrs of growth, cells were directly assayed in the liquid media using a BD LSRFortessa™ X-20 instrument. Fluoresceine Isothiocyanate (FITC) signal was collected using a 488 nm laser for excitation and a 515 – 545 nm bandpass filter for emission. About 50,000 events were collected on the cytometer and gated by forward and side scatter parameters to analyze single cells.

### **Yeast growth curves.**

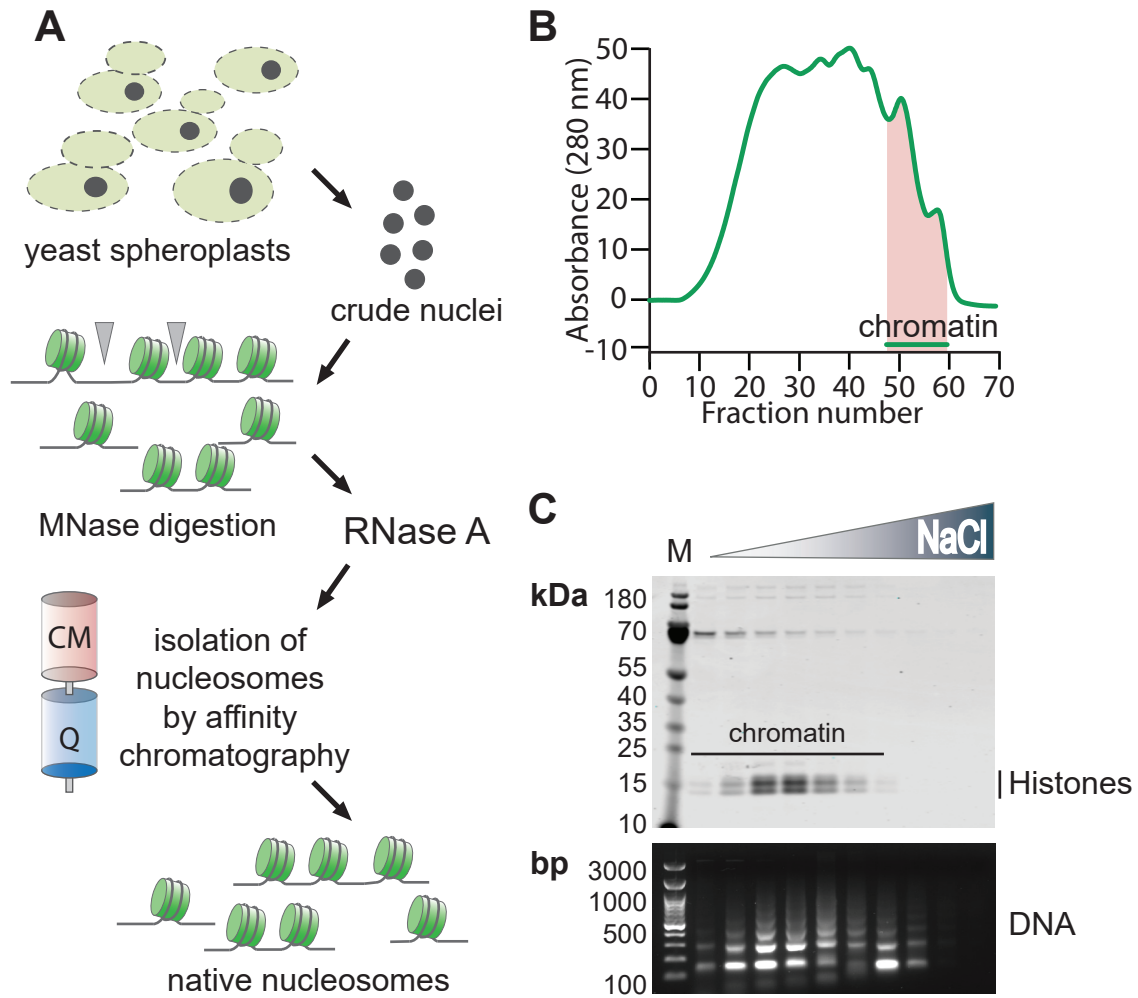
Yeast was inoculated from plate for a pre-culture in SC or SCEG without Zinc, in order to deplete intracellular zinc reserves. After 24 hrs, cells were diluted to OD<sub>600</sub> in the same media with the addition of 0.1 or 0.25  $\mu\text{M}$  ZnSO<sub>4</sub> (low zinc media) and, where indicated, additional CuSO<sub>4</sub>. 2.23  $\mu\text{M}$  ZnSO<sub>4</sub> was added for all replete zinc growth conditions.

Optical density was determined at indicated times using a SmartSpec 3000 (Biorad) spectrophotometer.

### **Acknowledgments**

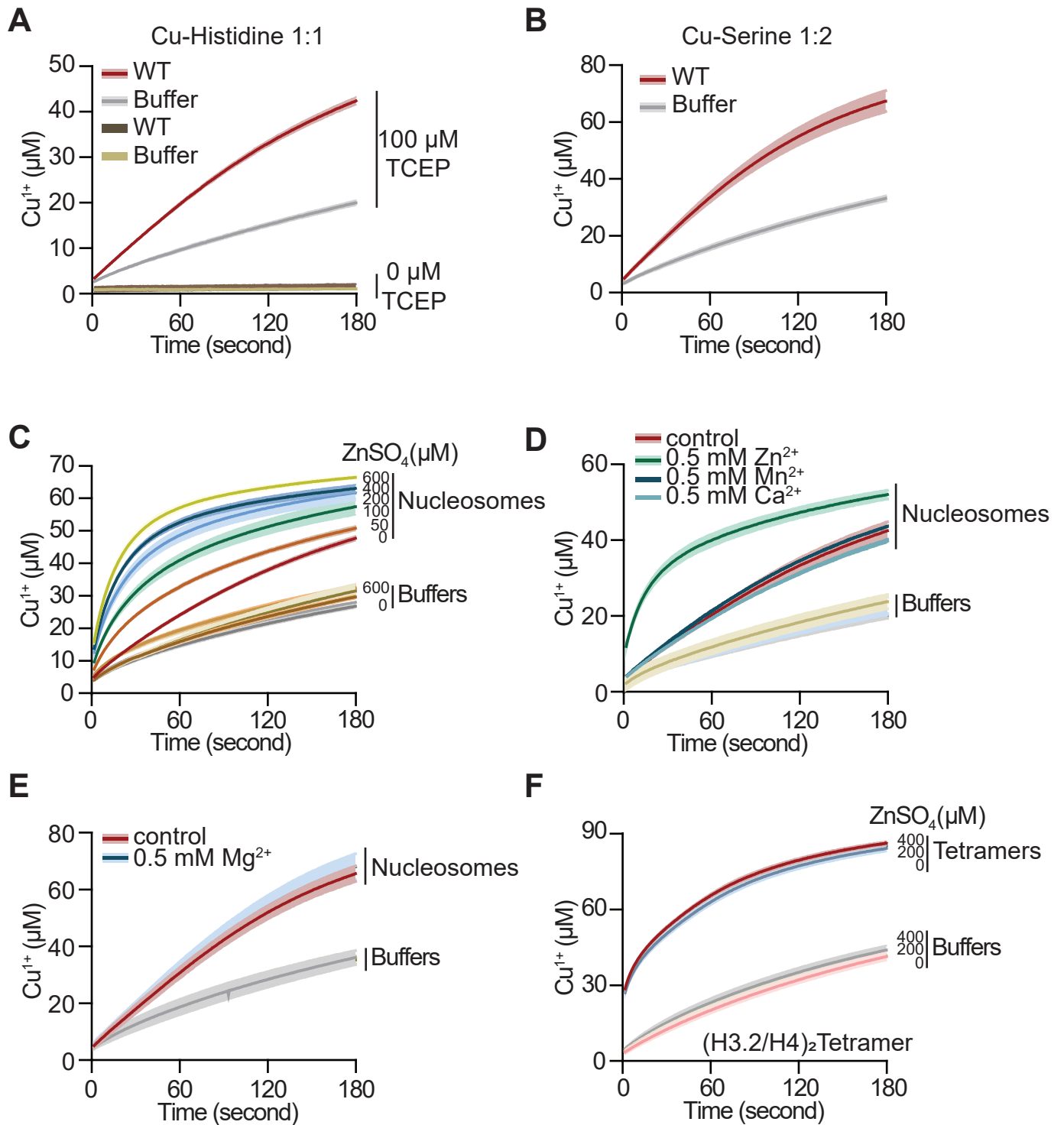
This study was supported by the NIH grant GM140106 and Moore-Simons Project on the Origin of the Eukaryotic Cell to SKK. Flow cytometry was performed in the UCLA Jonsson Comprehensive Cancer Center (JCCC) and Center for AIDS Research Flow Cytometry Core Facility that is supported by National Institutes of Health awards P30 CA016042 and 5P30 AI028697, and by the JCCC, the UCLA AIDS Institute, the David Geffen School of Medicine at UCLA, the UCLA Chancellor's Office, and the UCLA Vice Chancellor's Office of Research. We thank Craig L. Peterson for kindly providing the Lyticase expression plasmid pCP330, and all members of the Kurdistani lab for helpful discussions. We also thank Vijaya Pandey and James Wohlschlegel of the UCLA Proteome Research Center for mass spectrometry analyses.

Figure 1



**Figure 1. Isolation of native nucleosomes from the budding yeast.** A, Schematic overview of the protocol for isolating nucleosomal fragments from yeast cells. B, Representative sample chromatogram of the nucleosomal fragments eluted from anion exchange column. C, Representative example of eluted nucleosomal fractions (upper panel) and corresponding DNA (lower panel).

Figure 2



**Figure 2. Zinc is required for optimal yeast nucleosome copper reductase activity.**

A, Progress curves of  $\text{Cu}^{2+}$  reduction by WT nucleosomes or buffer in the presence or absence of the reducing agent TCEP and 1:1  $\text{Cu}^{2+}$ :histidine complex. Lines and shading represent the mean  $\pm$  standard deviation (SD) of three assays. B, Similar to A but using 1:2  $\text{Cu}^{2+}$ :serine complex as the substrate. C, Similar to A but with added specified quantities of  $\text{ZnSO}_4$ . D, Similar to A but in the presence of the indicated metals. Results from samples with  $\text{Mn}^{2+}$  and  $\text{Ca}^{2+}$  show the range from two assays. E, Similar to A but in the presence of  $\text{Mg}^{2+}$ . Note that unlike  $\text{Zn}^{2+}$ ,  $\text{Mn}^{2+}$ , the presence of  $\text{Ca}^{2+}$  or  $\text{Mg}^{2+}$  does not enhance the copper reductase activity of nucleosomes. F, Progress curves of  $\text{Cu}^{2+}$  reduction by the histone H3.2-H4 tetramer or buffer in the presence of the indicated amounts of  $\text{ZnSO}_4$ .

# Figure 3

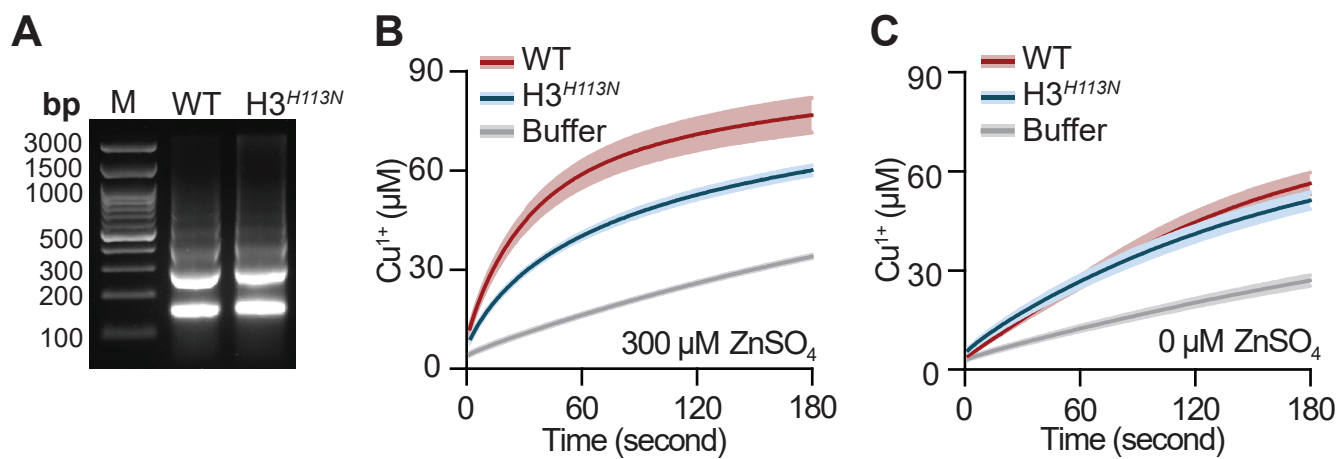


**Figure 3. Histone H3H113 is required for zinc stimulation of nucleosomal copper reduction.** A, Agarose gel electrophoresis of DNA from purified WT nucleosomes and those with the histone H3H113N mutation. B, Progress curves of  $\text{Cu}^{2+}$  reduction by WT nucleosomes, H3H113N mutant nucleosomes or buffer in the presence of 300  $\mu\text{M}$   $\text{ZnSO}_4$ . Lines and shading represent the mean  $\pm$  SD of three assays. C, Similar as B but in the absence of  $\text{ZnSO}_4$ .

Figure 4

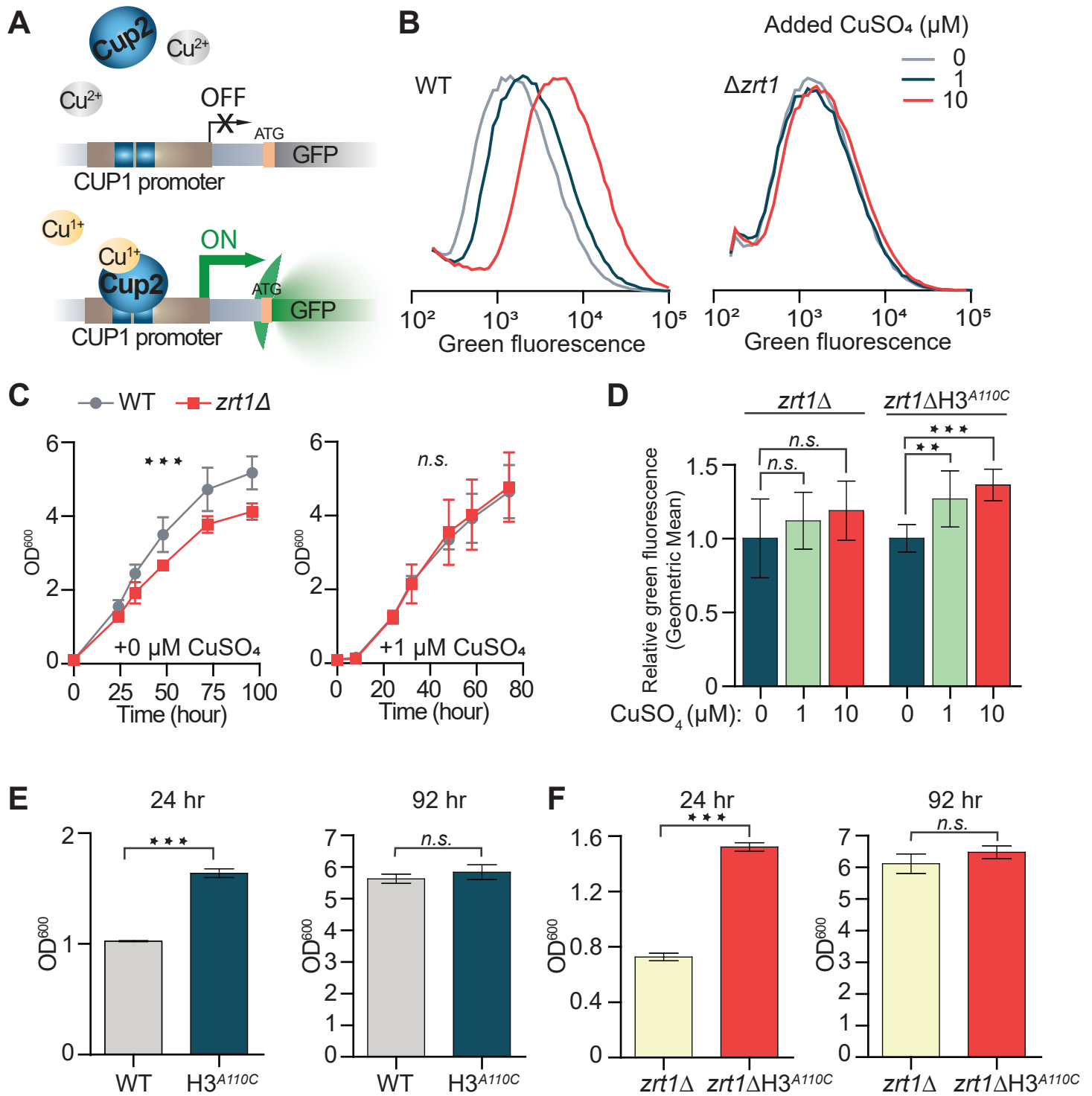


**Figure 4. Zinc is required for histone H3-mediated generation of Cu<sup>1+</sup> in cells.** A, Graphic depiction of the reporter assay used to evaluate intracellular Cu<sup>1+</sup> levels. B, Average flow cytometry distributions of WT or *zrt1Δ* cells containing the p<sup>(CUP1)</sup>-GFP plasmid, cultured in oxidative media lacking uracil (SCEG-ura) containing 0.25 μM ZnSO<sub>4</sub> in the absence (0) or presence of either 1 or 10 μM additional CuSO<sub>4</sub> from eight experiments. Baseline copper concentration in SCEG-ura is ~0.16 μM. C, Growth curves in SCEG media containing 0.1 μM ZnSO<sub>4</sub> without (0; left panel) or with 1 μM additional CuSO<sub>4</sub>. Lines show means at each time point ± SD derived from three experiments. The P value from a two-way ANOVA test is reported. D, Average relative geometric means of green fluorescence of *zrt1Δ* or *zrt1Δ* H3<sup>A110C</sup> cells containing the p<sup>(CUP1)</sup>-GFP plasmid cultured in SCEG-ura containing 0.25 μM ZnSO<sub>4</sub> in the absence (0) or presence of either 1 or 10 μM additional CuSO<sub>4</sub> from eight experiments. P-values were calculated using a two-tailed unpaired t-test. E, Growth after the indicated hours in SCEG in low zinc concentrations (0.1 μM ZnSO<sub>4</sub>). F, Growth after indicated hours of ZRT1 deletion strains (*zrt1Δ*) with either WT H3 or H3<sup>A110C</sup> in SCEG. Bars show mean optical density at OD600 ± SD derived from three experiments. P-values were calculated using a two-tailed unpaired t-test. \*\*\*P≤0.001; n.s. stands for “not significant”.

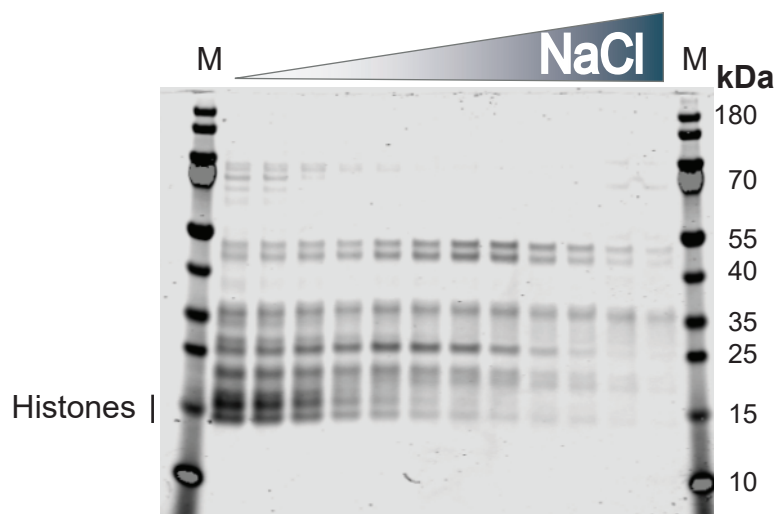
## References

1. Soshnev AA, Josefowicz SZ, & Allis CD (2018) Greater Than the Sum of Parts: Complexity of the Dynamic Epigenome. *Mol Cell* 69(3):533.
2. Laursen SP, Bowerman S, & Luger K (2021) Archaea: The Final Frontier of Chromatin. *J Mol Biol* 433(6):166791.
3. Attar N, *et al.* (2020) The histone H3-H4 tetramer is a copper reductase enzyme. *Science* 369(6499):59-64.
4. Campos OA, *et al.* (2021) A pathogenic role for histone H3 copper reductase activity in a yeast model of Friedreich's ataxia. *Sci Adv* 7(51):eabj9889.
5. Zhang Y, *et al.* (2006) Mrs3p, Mrs4p, and frataxin provide iron for Fe-S cluster synthesis in mitochondria. *J Biol Chem* 281(32):22493-22502.
6. Lill R & Freibert SA (2020) Mechanisms of Mitochondrial Iron-Sulfur Protein Biogenesis. *Annu Rev Biochem* 89:471-499.
7. Bulteau AL, *et al.* (2004) Frataxin acts as an iron chaperone protein to modulate mitochondrial aconitase activity. *Science* 305(5681):242-245.
8. Fazius F, Shelest E, Gebhardt P, & Brock M (2012) The fungal alpha-aminoadipate pathway for lysine biosynthesis requires two enzymes of the aconitase family for the isomerization of homocitrate to homoisocitrate. *Mol Microbiol* 86(6):1508-1530.
9. Brancaccio D, *et al.* (2017) [4Fe-4S] Cluster Assembly in Mitochondria and Its Impairment by Copper. *J Am Chem Soc* 139(2):719-730.
10. Macomber L & Imlay JA (2009) The iron-sulfur clusters of dehydratases are primary intracellular targets of copper toxicity. *Proc Natl Acad Sci U S A* 106(20):8344-8349.
11. Luger K, Mader AW, Richmond RK, Sargent DF, & Richmond TJ (1997) Crystal structure of the nucleosome core particle at 2.8 Å resolution. *Nature* 389(6648):251-260.
12. Grover P, Asa JS, & Campos EI (2018) H3-H4 Histone Chaperone Pathways. *Annu Rev Genet* 52:109-130.
13. Kuznetsov VI, Haws SA, Fox CA, & Denu JM (2018) General method for rapid purification of native chromatin fragments. *J Biol Chem* 293(31):12271-12282.
14. Mohideen K, Muhammad R, & Davey CA (2010) Perturbations in nucleosome structure from heavy metal association. *Nucleic Acids Res* 38(18):6301-6311.
15. Davey CA & Richmond TJ (2002) DNA-dependent divalent cation binding in the nucleosome core particle. *Proc Natl Acad Sci U S A* 99(17):11169-11174.
16. Wang Y, *et al.* (2018) The cellular economy of the *Saccharomyces cerevisiae* zinc proteome. *Metallomics* 10(12):1755-1776.
17. Maret W (2012) New perspectives of zinc coordination environments in proteins. (Translated from eng) *J Inorg Biochem* 111:110-116 (in eng).
18. Malavolta M, *et al.* (2015) Serum copper to zinc ratio: Relationship with aging and health status. *Mech Ageing Dev* 151:93-100.

19. Sakamoto M, *et al.* (2009) Global analysis of mutual interaction surfaces of nucleosomes with comprehensive point mutants. *Genes Cells* 14(11):1271-1330.
20. Dai J, *et al.* (2008) Probing nucleosome function: a highly versatile library of synthetic histone H3 and H4 mutants. *Cell* 134(6):1066-1078.
21. Ramachandran S, Vogel L, Strahl BD, & Dokholyan NV (2011) Thermodynamic stability of histone H3 is a necessary but not sufficient driving force for its evolutionary conservation. *PLoS Comput Biol* 7(1):e1001042.
22. Zhao H & Eide D (1996) The yeast ZRT1 gene encodes the zinc transporter protein of a high-affinity uptake system induced by zinc limitation. *Proc Natl Acad Sci U S A* 93(6):2454-2458.
23. Buchman C, Skroch P, Welch J, Fogel S, & Karin M (1989) The CUP2 gene product, regulator of yeast metallothionein expression, is a copper-activated DNA-binding protein. *Mol Cell Biol* 9(9):4091-4095.
24. Furst P, Hu S, Hackett R, & Hamer D (1988) Copper activates metallothionein gene transcription by altering the conformation of a specific DNA binding protein. *Cell* 55(4):705-717.
25. Butt TR, *et al.* (1984) Copper metallothionein of yeast, structure of the gene, and regulation of expression. *Proc Natl Acad Sci U S A* 81(11):3332-3336.
26. Karin M, *et al.* (1984) Primary structure and transcription of an amplified genetic locus: the CUP1 locus of yeast. *Proc Natl Acad Sci U S A* 81(2):337-341.
27. Thiele DJ (1988) ACE1 regulates expression of the *Saccharomyces cerevisiae* metallothionein gene. *Mol Cell Biol* 8(7):2745-2752.
28. Welch J, Fogel S, Buchman C, & Karin M (1989) The CUP2 gene product regulates the expression of the CUP1 gene, coding for yeast metallothionein. *Embo J* 8(1):255-260.
29. Macadangdang BR, *et al.* (2014) Evolution of Histone 2A for Chromatin Compaction in Eukaryotes. *Elife* 3.
30. Park S-Y & Kim J-S (2020) A short guide to histone deacetylases including recent progress on class II enzymes. *Experimental & Molecular Medicine* 52(2):204-212.
31. Maret W (2013) Zinc and the zinc proteome. *Met Ions Life Sci* 12:479-501.
32. Forman HJ & Fridovich I (1973) On the stability of bovine superoxide dismutase. The effects of metals. *J Biol Chem* 248(8):2645-2649.
33. Malasarn D, *et al.* (2013) Zinc deficiency impacts CO<sub>2</sub> assimilation and disrupts copper homeostasis in *Chlamydomonas reinhardtii*. *J Biol Chem* 288(15):10672-10683.
34. Aich P, *et al.* (1999) M-DNA: A complex between divalent metal ions and DNA which behaves as a molecular wire. *J Mol Biol* 294(2):477-485.
35. Langlais M, Tajmir-Riahi HA, & Savoie R (1990) Raman spectroscopic study of the effects of Ca<sup>2+</sup>, Mg<sup>2+</sup>, Zn<sup>2+</sup>, and Cd<sup>2+</sup> ions on calf thymus DNA: binding sites and conformational changes. *Biopolymers* 30(7-8):743-752.

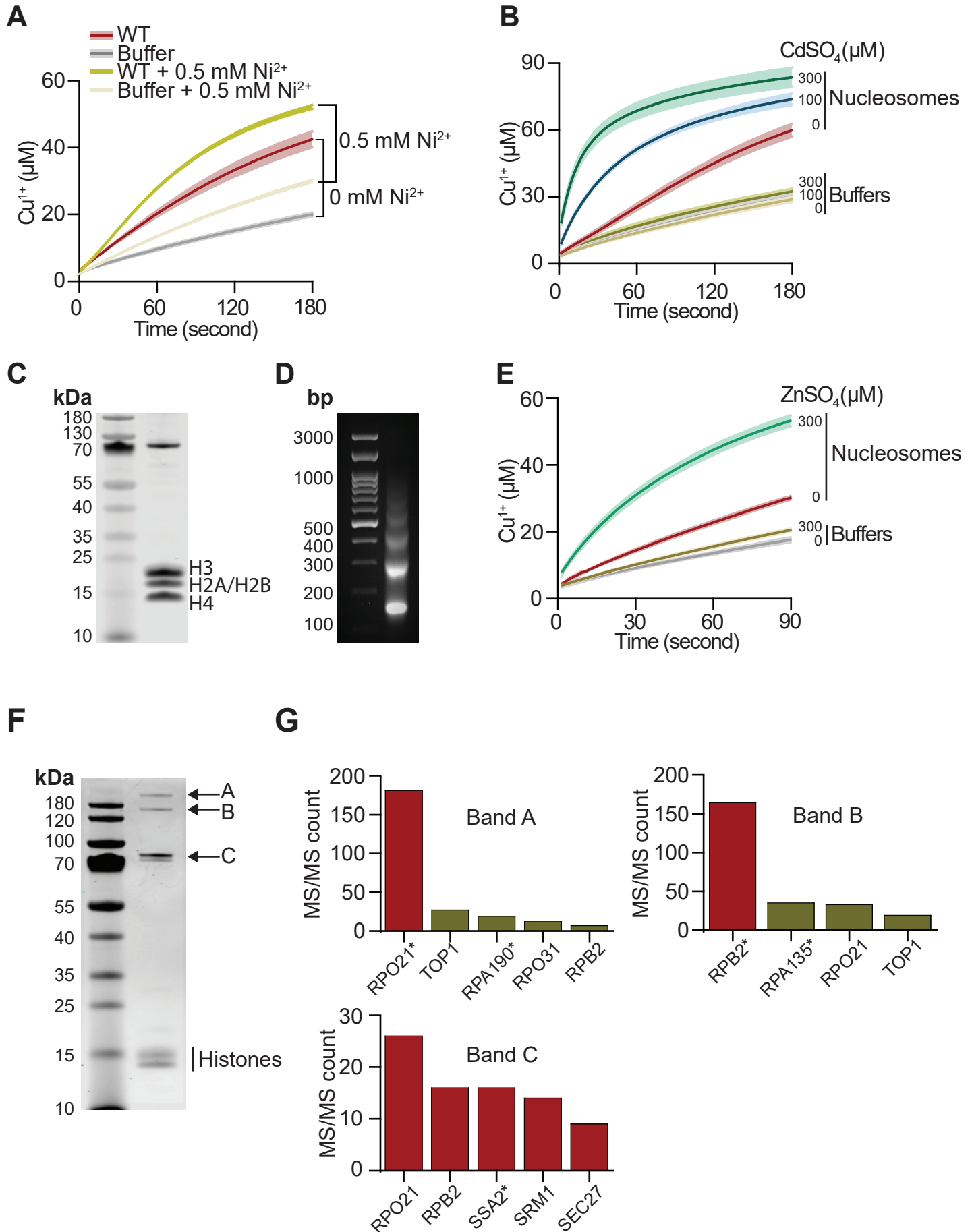
36. Lee JS, Latimer LJ, & Reid RS (1993) A cooperative conformational change in duplex DNA induced by Zn<sup>2+</sup> and other divalent metal ions. *Biochem Cell Biol* 71(3-4):162-168.
37. Adamczyk M, Poznanski J, Kopera E, & Bal W (2007) A zinc-finger like metal binding site in the nucleosome. *FEBS Lett* 581(7):1409-1416.
38. Ryan OW, *et al.* (2014) Selection of chromosomal DNA libraries using a multiplex CRISPR system. *Elife* 3.
39. Luger K, Rechsteiner TJ, & Richmond TJ (1999) Preparation of nucleosome core particle from recombinant histones. *Methods Enzymol* 304:3-19.
40. Luger K, Rechsteiner TJ, & Richmond TJ (1999) Preparation of nucleosome core particle from recombinant histones. *Method Enzymol* 304:3-19.
41. Shevchenko A, Wilm M, Vorm O, & Mann M (1996) Mass spectrometric sequencing of proteins silver-stained polyacrylamide gels. *Anal Chem* 68(5):850-858.
42. Jami-Alahmadi Y, Pandey V, Mayank AK, & Wohlschlegel JA (2021) A Robust Method for Packing High Resolution C18 RP-nano-HPLC Columns. *J Vis Exp* (171).
43. Cox J & Mann M (2008) MaxQuant enables high peptide identification rates, individualized p.p.b.-range mass accuracies and proteome-wide protein quantification. *Nat Biotechnol* 26(12):1367-1372.

# A Nucleosome purification without RNase A treatment



**Supplemental Figure 1. No RNase A step compromises the quality of purified native nucleosomes.** The coomassie-stained polyacrylamide gel electrophoresis (PAGE) of the eluted nucleosomal fractions. These were prepared as in figure 1C but without including the RNase A step.

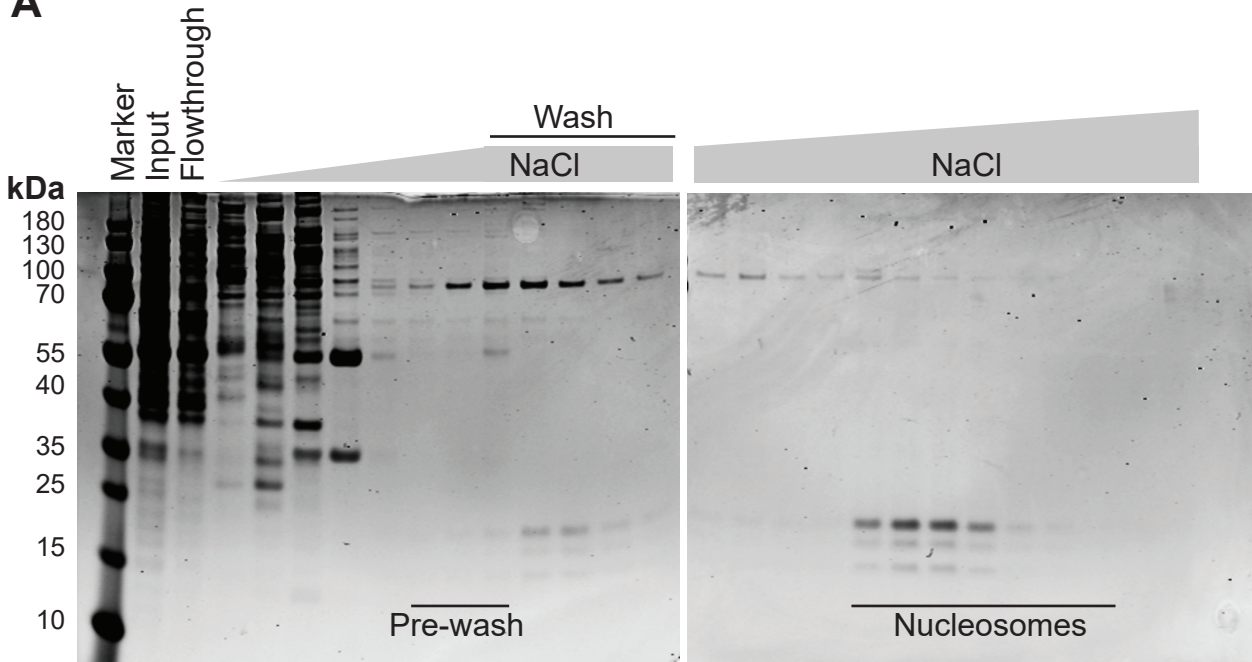
Figure S2



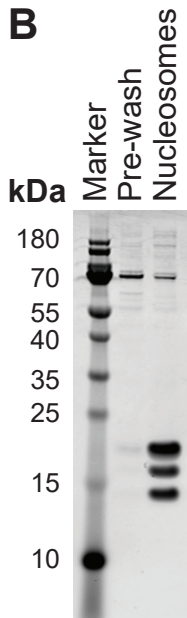
**Supplemental Figure 2. Enhancement of nucleosomal copper reduction is specific to zinc.** A, Progress curves of  $\text{Cu}^{2+}$  reduction by WT nucleosomes in the presence or absence of  $\text{Ni}^{2+}$ . The presence of  $\text{Ni}^{2+}$  primarily enhances non-specific  $\text{Cu}^{2+}$  reduction, as reflected by shifts in both buffer and nucleosome curves. Lines and shading represent the mean  $\pm$  SD of two or three assays. B, Progress curves of  $\text{Cu}^{2+}$  reduction by WT nucleosomes in the presence of indicated  $\text{Cd}^{2+}$  concentrations. Lines and shading represent the mean  $\pm$  SD of three assays. C, Coomassie staining of nucleosomes prepared from spheroplasts obtained using recombinant Lyticase. D, DNA of the nucleosomes from C. E, Progress curves of  $\text{Cu}^{2+}$  reduction by nucleosomes obtained from spheroplasts prepared with recombinant Lyticase or buffer with addition of the indicated amounts of  $\text{ZnSO}_4$ . Lines and shading represent the mean  $\pm$  SD of three assays. F, PAGE of a representative sample of purified nucleosomes. The major co-eluting bands are labeled (A, B, and C). G, Bar graphs show the quantitation (normalized MS/MS count) of peptides identified through mass spectrometry analysis of each co-eluting band as labeled in F. Proteins matching in size of the indicated bands are denoted with an asterisk.

Figure S3

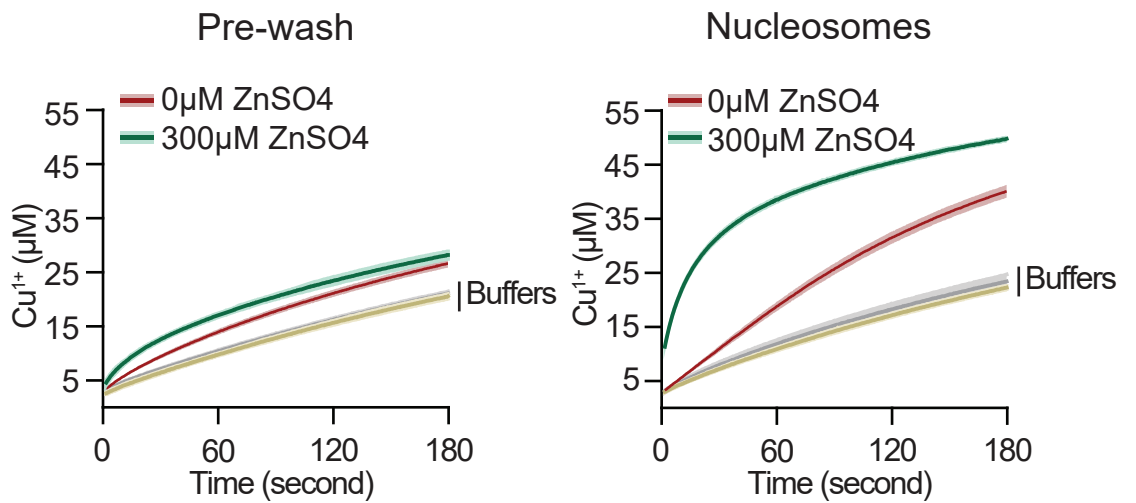
**A**



**B**

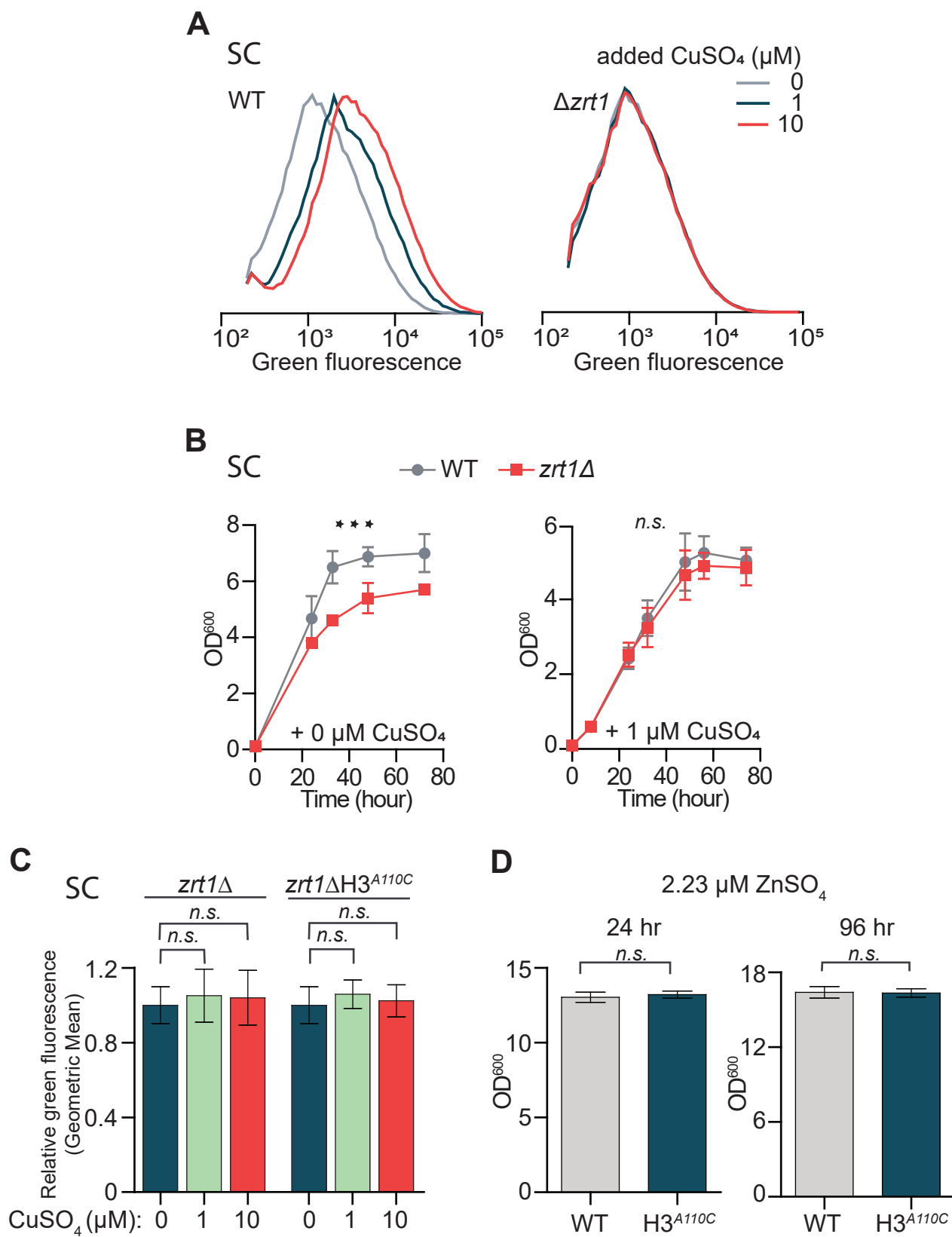


**C**



**Supplemental Figure 3. Copper reductase activity copurifies with nucleosomes.** A, Coomassie-stained PAGE analysis of fractions eluted by a salt gradient after a high-salt wash step. The initial gradient, ranging from 300 to 572 mM NaCl, is followed by two column volumes of 568 mM NaCl (left gel). Nucleosomes are then eluted in a subsequent gradient from 568 to 700 mM NaCl (right gel). Fractions pooled as “Pre-wash” and “Nucleosomes” samples are indicated. B, Coomassie-stained PAGE analysis of pooled “Pre-wash” and “Nucleosomes” fractions. C, Progress curves of Cu<sup>2+</sup> reduction by the pooled samples shown in B. Lines and shading represent the mean ± SD of three assays.

Figure S4



**Supplemental Figure 4. Zinc is required for histone H3-mediated generation of**

**Cu<sup>1+</sup> in cells.** A, Average green fluorescence distributions of WT or *zrt1Δ* cells containing the p<sup>(CUP1)</sup>-GFP plasmid cultured in fermentative media lacking uracil (SC-ura) containing 0.25 μM ZnSO<sub>4</sub>, in the absence (0) or presence of either 1 or 10 μM additional CuSO<sub>4</sub> from eight experiments. B, Growth curves in fermentative SC media containing 0.25 μM ZnSO<sub>4</sub>, in the absence (0; left panel) or presence 1 μM additional CuSO<sub>4</sub>. Lines show means at each time point ± SD from three experiments. The P value from a two-way ANOVA test is reported. \*\*\*P≤0.001; n.s. stands for “not significant”. C, Average relative geometric means of green fluorescence *zrt1Δ* or *zrt1Δ* H3<sup>AI10C</sup> cells containing the p<sup>(CUP1)</sup>-GFP plasmid cultured in SC-ura containing 0.25 μM ZnSO<sub>4</sub>, in the absence (0) or presence of either 1 or 10 μM additional CuSO<sub>4</sub> from eight experiments. P-values were calculated using a two-tailed unpaired t-test. n.s. stands for “not significant”. D, Growth after the indicated hours in SCEG in replete zinc concentrations (2.23 μM ZnSO<sub>4</sub>). P-values were calculated using a two-tailed unpaired t-test. n.s. stands for “not significant”.